

were  $\leq 5$  s, given the sensitivity ( $\sim 0.02$  dB) and instrumental time constant ( $\sim 0.1$  s) that can be achieved with riometers. Ionospheric time constants of this order may apply in the  $D$  region during absorption events associated with some magnetic storms and substorms.

The research at the University of Maryland was supported by NSF grants DPP74-01704, DPP76-82041 and ATM77-22937. Additional support for balloon operations in Canada was provided by the Office of Naval Research (contract N00014-67-A-0239-0033). Bell Laboratories acknowledge the NSF for logistics support for the Siple measurements. We thank Dr H. Chivers for cooperation in the riometer data acquisition.

Received 4 September; accepted 13 November 1979.

1. Chivers, H. J. A. & Maagoe, S. *IEEE Trans. on Antennas and Propagat.* **513**, July (1972).
2. Lanzerotti, L. J., MacLennan, C. G. & Evans, C. J. *geophys. Res.* **83**, 2525 (1978).
3. Lanzerotti, L. J., Hasegawa, A. & Tartaglia, N. A. *J. geophys. Res.* **77**, 6731 (1972).
4. Leavitt, M. K., Carpenter, D. L., Seely, N. T., Padden, R. R. & Doolittle, J. H. *J. geophys. Res.* **83**, 1601 (1978).
5. Fukunishi, H. & Lanzerotti, L. J. *J. geophys. Res.* **79**, 4632 (1974).
6. Rosenberg, T. J., Foster, J. C., Matthews, D. L., Sheldon, W. R. & Benbrook, J. R. *J. geophys. Res.* **82**, 177 (1977).
7. Bering, E. A. *et al.* *J. geophys. Res.* **84**, (in press).
8. Reid, J. S. & Phillips, J. *Planet Space Sci.* **19**, 959 (1971).
9. Roldugin, V. K. *Geomagn. Aeron.* (English translation) **7**, 454 (1967).
10. Siren, J. C., Rosenberg, T. J., Detrick, D. & Lanzerotti, L. J. *J. geophys. Res.* (submitted).

## Charge dependence of pion production in heavy ion collisions

G. Bertsch

Department of Physics and Cyclotron Laboratory,  
Michigan State University, East Lansing, Michigan 48824

Benenson *et al.*<sup>1</sup> measured the pion production cross-section in nuclear heavy ion collisions in the energy range 100–400 MeV per nucleon with the aim of determining whether collective effects associated with the larger number of nucleons were present in the pion field. An instability in the pion field, such as the putative pion condensation phase transition<sup>2</sup>, would give rise to an enhanced number of physical pions. The expected production cross-section, in the absence of collective effects, is found from two simple models. One of these is a statistical model, in which the number of pions is calculated from a statistical equilibrium. At the other extreme, the nucleons in the target and projectile are assumed to be free and independent, except for their Fermi momentum, and create pions by two-body collisions. The experimental cross-section at the lowest energy was found to be larger than either model by at least an order of magnitude<sup>3</sup>, suggesting that collective effects are indeed present. Interestingly, the cross-section had unexpectedly strong dependence on the charge of the pion produced. At the highest energy studied, 400 MeV per nucleon, many more  $\pi^-$  than  $\pi^+$  were produced in the forward direction. At the lowest energy studied, 100 MeV per nucleon, the relative yields are reversed, with more  $\pi^+$  produced. The experimental ratios of  $\pi^-$  to  $\pi^+$ ,

$$R_{-/+} = \frac{d\sigma_{\pi^-}}{d^3p} / \frac{d\sigma_{\pi^+}}{d^3p}$$

are quoted in Table 1. Benenson *et al.*<sup>1</sup> explain the  $\pi^-$  enhancement in terms of the Coulomb distortions of the pion wavefunctions. Here I include in the same framework an explanation of the low energy result.

My starting point for the pion production rate is the formula

$$W = 2\pi \sum_i \langle i | H_{\pi N} | f \rangle^2 \rho_i$$

**Table 1** Experimental ratios of  $\pi^-$  to  $\pi^+$

$E_{\text{proj}}$ (MeV per nucleon)	Pion kinetic energy (MeV)	$y_{\pi^-} - y_{\text{proj}}^*$	$R_{-/+}$
~100	34	0.23	0.7
	54	0.40	0.6
	76	0.54	0.5
400	34	-0.20	3.0
	54	-0.04	10.0
	76	0.11	2.5
	123	0.36	1.4
	155	0.49	1.2

\* Rapidity, the Lorentz-additive measure of velocity, is defined as  $y = \frac{1}{2} \ln(E + pc)/(E - pc)$ .

where  $\rho_i$  is the density of final states and  $H_{\pi N}$  is the pion creation part of the nuclear hamiltonian. The  $\rho_i$  is a product of density of pionic states  $\rho_i^\pi$ , and density of nucleonic states  $\rho_i^N$ . Normalising the pion wavefunction to plane waves at infinity, the pionic

density of states is the usual  $\rho_i^\pi = \frac{d^3p}{(2\pi)^3}$ . The transition matrix element  $\langle i | H_{\pi N} | f \rangle^2$  will be proportional to the probability of these normalised wavefunctions in the collision region,  $|\phi_{\pi^*}|^2$ . Benenson *et al.*<sup>1</sup> compute the charge dependence as

$$R_{-/+} \approx \frac{|\phi_{\pi^-(R)}|^2}{|\phi_{\pi^+(R)}|^2}$$

where  $\phi_{\pi^*}$  contains the Coulomb distortion of the projectile. Thereby the large effect seen for pion velocities close to the beam velocity is qualitatively explained. The effect of the nuclear density of states will now be included. To describe  $\rho_i^N$ , it is assumed that there is a thermal equilibrium among nucleons. The final state density then depends on pion energy and charge according to

$$\rho_i^N \sim \exp[-(E_{\pi^*} \mp (\mu_p - \mu_n))/kT] \quad (1)$$

Here  $kT$  is the temperature of the nucleons, and  $\mu_p$  and  $\mu_n$  are the chemical potentials of the protons and neutrons. In view of the relatively small number of nucleons involved in the collision, and the fact that the pions are most likely to be created at the initial stages of the collision, before any sort of equilibrium is established, the statistical assumption may be questioned. However, it is a fact that energy spectra tend to be exponential, with a coefficient close to the 'temperature' calculated as below<sup>4</sup>. Thus we at least find phenomenological justification for equation (1).

$R_{-/+}$  is now compared at the two energies, for the same velocity of the pion with respect to the projectile. The Coulomb distortion effects should be nearly the same, so the ratio of  $R_{-/+}$  would be given by

$$R_{-/+}/R'_{-/+} \approx \exp \left[ 2(\mu_p - \mu_n) \left( \frac{1}{kT'} - \frac{1}{kT} \right) \right]$$

In the system studied experimentally,  $^{20}\text{Ne} + \text{NaF}$ , the chemical potentials differ mainly because of the Coulomb field. Assuming that the pion production takes place in an overlap region between the colliding nuclei, the difference between chemical potentials may be estimated as

$$\mu_p - \mu_n = \frac{Ze^2}{R} \approx \frac{20(1.44)}{3.3} \text{ MeV} \approx 8.7 \text{ MeV}$$

To estimate the temperature at 100 MeV per nucleon projectile energy, note that the energy available in the centre of mass, per nucleon, is  $\sim 25$  MeV. With Boltzmann statistics, this implies a temperature of  $\frac{2}{3}(25) = 16.7$  MeV. A more detailed calculation taking into account such things as quantum statistics and binding energy effects yields a temperature of 13.5 MeV. Similar considerations for 400 MeV per nucleon yield a temperature of

55 MeV. Then for a given pion velocity with respect to the projectile, we expect a diminution of  $\pi^-$  at the lower energy of

$$R/R' \approx \exp\left(17.4\left(\frac{1}{55} - \frac{1}{13.5}\right)\right) \approx 0.37$$

This agrees with the experimental ratio  $0.5/1.2 \approx 0.42$  found for pions of high rapidity.

From these considerations, it seems that  $R_{-/+}$  will be a useful probe of the nucleonic density of states in the early stages of heavy ion collisions at lower bombarding energies, and seems to be conveniently interpretable as a temperature. This complements the usefulness of  $R_{-/+}$  at higher energies as a probe of the geometry of the collisions, via the dependence on the Coulomb distortions.

I thank W. Benenson for discussions, and the NSF for support under grant no. PHY-7620097.

Received 18 September; accepted 22 November 1979.

1. Benenson, W. *et al.* *Phys. Rev. Lett.* **43**, 683–686 (1979).
2. Migdal, A. B. *et al.* *Rev. mod. Phys.* **50**, 107–172 (1978).
3. Benenson, W. *et al.* *Phys. Rev. Lett.* (in the press).
4. Siemens, P. J. & Rasmussen, J. O. *Phys. Rev. Lett.* **42**, 880–883 (1979).

## Improved planar solar convertor based on uranyl neodymium and holmium glasses

Renata Reisfeld & Yehoshua Kalisky

Department of Inorganic Chemistry and Energy Center, The Hebrew University, Jerusalem, Israel

The use of uranyl doped glasses for solar energy conversion and concentration was discussed by Reisfeld and Neuman<sup>1</sup>. While the  $\text{UO}_2^{2+}$  ion is an efficient energy convertor, its maximum emission peaking around 500 nm does not coincide with the maximum sensitivity of the existing solar cells which is around 700–1,000 nm. The use of  $\text{Nd}^{3+}$  doped glasses for solar energy collectors was described by Levitt and Weber<sup>2</sup>. While the emission of  $\text{Nd}^{3+}$  peaking at 880 nm ( $^4\text{F}_{3/2} \rightarrow ^4\text{I}_{9/2}$ ) and at 1.06  $\mu\text{m}$  ( $^4\text{F}_{3/2} \rightarrow ^4\text{I}_{11/2}$ ) is ideal for matching with the maximum sensitivity of solar cells, its absorbance arising from the forbidden transition  $4f-4f$  is low and the overlap of the absorption spectrum of  $\text{Nd}^{3+}$  with the solar spectrum is rather weak. To increase the operational efficiency of solar collectors, a maximum overlap between the absorption spectrum of the collector and the solar spectrum is required<sup>3</sup>. In this report we suggest that glasses doped by uranyl and neodymium and uranyl and holmium increase the response to the solar spectrum, thus increasing the collection efficiency, and convert the absorbed light in the wide spectral range into the narrow fluorescence band at 1.06  $\mu\text{m}$  and 880 nm in uranyl-neodymium glasses and 660 nm ( $^5\text{F}_5 \rightarrow ^5\text{I}_8$ ) and 750 nm ( $^5\text{F}_4, ^5\text{S}_2 \rightarrow ^5\text{I}_7$ ) in the uranyl-holmium co-doped glasses.

Energy transfer from  $\text{UO}_2^{2+} \rightarrow \text{Nd}^{3+}$  in barium crown glasses was discussed by Gandy *et al.*<sup>4</sup> and Melamed *et al.*<sup>5</sup> for small concentrations of  $\text{UO}_2^{2+}$  in the glasses. The use of energy transfer for lowering the laser threshold in rare earth doped glasses is a well-known phenomenon<sup>6</sup>. Here we present quantitative calculations on energy transfer between  $\text{UO}_2^{2+} \rightarrow \text{Nd}^{3+}$  and  $\text{UO}_2^{2+} \rightarrow \text{Ho}^{3+}$  at a much higher concentration range than in ref. 4. This higher concentration range is suitable for solar energy conversion. The absorption, excitation and emission spectrum of  $\text{UO}_2^{2+}$  doped phosphate glasses may be found in ref. 1.

The excitation spectrum of the  $^4\text{F}_{3/2} \rightarrow ^4\text{I}_{11/2}$  (1.06  $\mu\text{m}$ ) transition of a glass doped by 2 wt %  $\text{Nd}^{3+}$  and co-doped by 2 wt %  $\text{Nd}^{3+}$  + 1 wt %  $\text{UO}_2^{2+}$  in the spectral range 360–500 nm

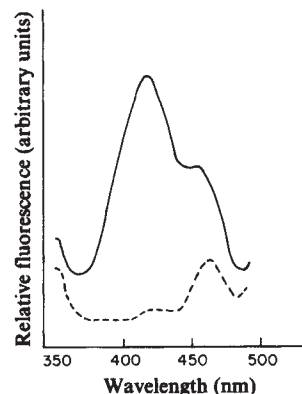


Fig. 1 Excitation of  $\text{Nd}^{3+}$  (---) and  $\text{Nd}^{3+} + \text{UO}_2^{2+}$  (—). Emission monitored at 1,055 nm.

is presented in Fig. 1. Due to the energy transfer from  $\text{UO}_2^{2+}$  to  $\text{Nd}^{3+}$ , the integrated fluorescence intensity of  $\text{Nd}^{3+}$  excited in this region is increased 8.5-fold. In the total spectral range from 360–800 nm this increase amounts to 150%. This percentage is equal to the number of photons of the solar spectrum affecting the co-doped glass divided by the number of photons affecting the  $\text{Nd}^{3+}$ -only doped glass. This ratio was calculated using the formula:

$$\frac{S_{\text{cod}}}{S_{\text{dop}}} = \frac{A^1 \times \eta_{\text{tr}} \times \eta^1 + A^2 \times \eta^2}{A^2 \times \eta^2} \times 100 \quad (1)$$

Where  $S_{\text{cod}}$  is area under the excitation spectrum of the co-doped glass, and  $S_{\text{dop}}$  the area under the excitation spectrum of the  $\text{Nd}^{3+}$  doped glass. The area of the excitation spectrum was corrected for the spectral response of the xenon source and the excitation monochromator.  $\eta_{\text{tr}}$  is energy transfer efficiency from  $\text{UO}_2^{2+}$  to  $\text{Nd}^{3+}$ ,  $A^1$ ,  $A^2$  = absorbance of  $\text{UO}_2^{2+}$  and  $\text{Nd}^{3+}$  respectively, and  $\eta^1$ ,  $\eta^2$  = fluorescence quantum efficiency of  $\text{UO}_2^{2+}$  and  $\text{Nd}^{3+}$  respectively.

The emission spectrum of  $\text{Nd}^{3+}$  and  $\text{Ho}^{3+}$  glasses co-doped with  $\text{UO}_2^{2+}$  are presented in Fig. 2. The emission maxima correspond to the maximum sensitivity of the silicon solar cells<sup>7</sup>. The efficiency of energy transfer was calculated using equations (2) and (3) and is presented in Table 1.

$$\eta_{\text{tr}} = 1 - \frac{\tau_d}{\tau_d^0} \quad (2)$$

$$\eta_{\text{tr}} = 1 - \frac{I_d}{I_d^0} \quad (3)$$

Where  $\tau_d$  is the first  $e$ -folding time<sup>6</sup> of  $\text{UO}_2^{2+}$  in the presence of  $\text{Nd}^{3+}$  and  $\tau_d^0$  is the first  $e$ -folding time of  $\text{UO}_2^{2+}$  alone.  $I_d$  and  $I_d^0$

Fig. 2 Fluorescence emission spectra of  $\text{Nd}^{3+}$  and  $\text{Ho}^{3+}$  co-doped with  $\text{UO}_2^{2+}$  when excited into the maximum absorption peak of  $\text{UO}_2^{2+}$ .

